An Examination of the Oxygen Reduction Reaction on RuO$_2$-based Oxide Coatings Formed on Titanium Substrates

Yoshio TAKASU,* Kyosuke OOHORI, Norihiro YOSHINAGA

and Wataru SUGIMOTO

Department of Fine Materials Engineering, Faculty of Textile Science and

Technology, Shinshu University, 3-15-1 Tokida, Ueda 386-8567, Japan

Abstract

The RuO$_2$-based electrocatalysts were prepared by using a dip-coating method on Ti plate substrates at 400 °C. The catalytic activity of the oxide-coated electrodes for the oxygen reduction reaction (ORR) was evaluated by cyclic voltammetry in 0.5 M H$_2$SO$_4$ at 60 °C in a stationary state. The examination was focused on the enhancement of the catalytic activity in the reaction by the enlargement of the surface area of the RuO$_2$ coating with the help of lanthunum. The onset potential for the ORR, $E_{\text{ORR-0}}$, of the RuO$_2$/Ti electrode showed that the highest value was 0.84 V vs. RHE.

1. Introduction

Platinum-based alloys are presently the typical cathode catalysts used for Polymer Electrolyte Fuel Cells (PEFCs) due to their high oxygen reduction activity. Since platinum is a highly expensive material, the development of catalysts to replace platinum, including oxides [1-3], carbides [4,5], and metal complexes [6,7], etc., has widely been examined by many research groups. Recently, some interesting studies on the development of Pt-free oxide cathodes, such as $TaO_{0.92}N_{1.05}$ and ZrO_{2-x}, have been reported [8,9]. Although these and numerous other studies have significantly contributed to the development of PEFC and DMFC, further investigation is still required for the improvement of both activity and durability. The RuO_2-TiO_2/Ti binary and IrO_2-RuO_2-TiO_2/Ti ternary oxide electrodes are widely used as the Dimensionally Stable Anode (DSA$^{®}$) catalyst-electrode in the electrolysis process for chlorine production in chlor-alkali industries [10]. Although basic investigations of the ORRs of ruthenium metal and compounds in acidic solutions have been published [11-14], few reports on crystalline ruthenium oxide in acidic solutions have been published [15].

This study presents a fundamental investigation of the development of non-Pt catalyst cathodes for PEFCs, using RuO_2-based oxides which were coated on a Ti plate substrate. This investigation using ruthenium oxide as the cathode is the first-step towards the development of less expensive and anti-corrosive oxide cathodes in the future.

2. Experiment

2.1. Preparation of RuO_2/Ti electrodes by a dip-coating method

Rutile-type RuO_2 coating-film was prepared on a Ti plate ($10 \times 10 \times 1$ mm) substrate by a conventional dip-coating method using a ethylene glycol solution of ruthenium chloride ($[RuCl_3] = 0.5$ M). The titanium substrates were etched with 10% oxalic acid at 80°C for 1 h, and then rinsed with deionized water before the dipping procedure. Calcination of the dip-coated salts was conducted in air at 400 °C. The dip-drying/calcination (alernating 10 min each) procedure was repeated 10 times. RuO_2/Ti electrodes with extremely enlarged surface areas were prepared using a dip-coating solution containing $RuCl_3$ and $LaCl_3$ in ethylene glycol ($[RuCl_3] = [LaCl_3] = 0.5$ M) [16, 17]. After the dip-drying/calcination (400 °C, 10 min) procedure was repeated 10 times, any of the lanthanum species were removed with 0.5 M H_2SO_4 at 80 °C. According to the Energy Dispersive X-ray Fluorescence Spectroscopy (EDX) analysis, the complete removal of the La_2O_3 by the acid treatment was confirmed. This electrode was denoted as the La_2O_3-treated RuO_2/Ti electrode in this study.

Individual oxides: RuO_2 and binary oxides of RuO_2 mixed with either MoO_x and VO_x were also prepared on Ti substrates by a dip-coating method using ethylene glycol solutions of metal salts: $RuCl_3$, $MoCl_5$ and $VOCl_3$. Calcination of the dip-coated salts was conducted at 400°C in air. The dipping-drying-calcination procedure was repeated 10 times in order to prepare electrodes that showed reproducible performance. These oxide electrodes are denoted as the RuO_2/Ti, $RuMo(1:1)O_x$/Ti and $RuV(1:1)O_x$/Ti electrodes.

2.2. Electrochemical measurements

The ORR activity of the oxide electrodes was evaluated by cyclic voltammetry (CV) in 0.5 M H_2SO_4 using a beaker-type electrolytic cell (Fig. 1), in a stationary state at 60 °C.

A carbon felt, rather than Pt, was used as the counter electrode in order to avoid the deposition of Pt onto the test electrode through dissolution. Although an Ag/AgCl reference electrode was used, the electrode potential is presented vs RHE. A Luggin capillary faced the working electrode at a distance of 2 mm. All electrode potentials are referred to the RHE(t) scale, corrected for temperature effect. For the ORR experiment, oxygen gas was bubbled into the 0.5 M H_2SO_4 solution at 60 °C.

3. Results and discussion

3.1 ORR activity of RuO$_2$/Ti electrodes enhanced by the morphological modification of the oxide layers

Figure 2-(a) shows CVs of the RuO$_2$/Ti electrode in N$_2$-saturated 0.5 M H_2SO_4 (dotted line) and in O$_2$-saturated 0.5 M H_2SO_4 (solid line). During both potential scans (anodic and cathodic potential sweeps), an additional cathodic current was observed for the CV measured with an O$_2$-saturated solution, as compared with the measured with an N$_2$-saturated solution. This additional cathodic current is due to the ORR on the oxide electrode. In order to enhance the ORR activity of this oxide electrode, we have tried to use lanthunum to enlarge the surface area of the oxide [16,17]. When a DSA-type binary oxide electrode was prepared with a dip-coating solution containing ruthenium salt and a rare earth salt, the resulting electrode was composed of a composite oxide of each element so long as the calcination temperature was not too high. Since the rare earth oxide can easily be removed by acid, a porous RuO$_2$ layer with an extremely enlarged surface area remained after the acid treatment of the composite electrode. Figure 2-(b) shows CVs of the La$_2$O$_3$-treated

4

$RuO_2(Ru:La=1:1)/Ti$ electrode in N_2-saturated 0.5 M H_2SO_4 (dotted line) and in O_2-saturated 0.5 M H_2SO_4 (solid line). Obviously, the pseudocapacitance of the La_2O_3-treated $RuO_2(Ru:La=1:1)/Ti$ electrode, (b), is much higher than that of the RuO_2/Ti electrode, (a). To clarify the enhancement effect of the La_2O_3-treatment, the molar ratio of La to Ru in the dip-coating solution was changed, and the ORR behaviors of those electrodes were evaluated. Figure 3 shows the ORR cathodic current curves for the electrodes presented in each geometric surface area, which were obtained by subtracting the voltammogram of the O_2-saturated solution during a cathodic scan from that of the N_2-saturated electrolytes. Since the voltammetry was carried out under a stationary state, the ORR current densities of these electrodes must be compared carefully. However, it can be said that the cathodic current and the E_{ORR-0} for the ORR increases with an increase in the molar ratio of La to Ru. The onset electrode potential, E_{ORR-0}, for the ORR is defined by the potential where the additional cathodic current begins to be observed on the voltammogram, and that of E_{ORR-20} is the potential where the additional cathodic current attained to 20 $\mu A/cm^2$-(geometric). The onset electrode potentials for the ORR on RuO_2/Ti, $RuO_2(Ru:La=9:1)/Ti$, $RuO_2(Ru:La=7:3)/Ti$ and $RuO_2(Ru:La=1:1)/Ti$ are listed in Table 1. Among these electrodes, the $RuLa(1:1)O_2/Ti$ electrode showed the highest activity for the ORR.

The La_2O_3-treated RuO_2/Ti electrodes which were prepared with much more lanthunum content than 1:1 were unstable after the dissolution of La_2O_3 from the RuO_2-La_2O_3 composite oxide layers in acid. The RuO_2/Ti electrode, (a), prepared by this dip-coating method showed typical surface morphology as shown in Fig. 4-(a). As shown in the four High Resolution Scanning Electron Microscopy (HRSEM) images in Fig. 4, the size of the RuO_2 particles decreased

with an increase in the molar ratio of La to Ru. Qualitatively, it could be said that the reason that the increase in the catalytic activity of the RuO$_2$/Ti electrode for the ORR increases with the La to Ru ratio is accounted for by the increase of the surface area of the porous RuO$_2$ layers. As shown in the X-ray diffraction (XRD) patterns of the RuO$_2$/Ti and the RuO$_2$(Ru:La=1:1)/Ti electrodes shown in Fig. 5, rutile-type RuO$_2$ was formed on the Ti substrate under the preparation conditions. The difference of the particle size of RuO$_2$ shown in Fig. 4 reflects both on the peak intensity and the half width of the diffraction patterns of these electrodes. Thus, the crystallite size of the RuO$_2$ of the latter electrode is also smaller than that of the former electrode. Although the XRD pattern of the latter electrode was taken after the dissolution of lanthunum species in the oxide layer by acid, an unknown peak was observed around $2\theta = 43.8°$. The possibility of the formation of a small amount of a ruthenium compound with lanthunum can not be excluded, while lanthunum was not detected by the EDX.

3.2 ORR activity of RuO$_2$/Ti electrodes enhanced by the addition of other elements

Since both IrMoO$_2$/Ti and IrVO$_2$/Ti showed a high activity for the ORR as reported in the previous paper [18], the effect of the addition of either molybdenum or vanadium to RuO$_2$ was examined. For the binary electrodes, RuMo(1:1)O$_2$/Ti and RuV(7:3)O$_2$/Ti, most of the molybdenum and vanadium remained in each of the oxide layers even after the HCl treatment at 80 °C. As shown in Fig. 6, the enhancement effect of the addition of these elements to RuO$_2$ was not so great, so long as the content ratios. In the previous paper concerning the enhancement of the ORR activity of the IrO$_2$/Ti electrode, we confirmed that the following two methods are effective for the oxide catalyst

electrode: the first method is the formation of a solid solution to change the valency of iridium ions with another element [18], and the second method is the use of rare earth elements to enlarge the surface area of oxides [16,17]. However, the first effect was moderate for the RuO_2-based electrode in comparison with the IrO_2-based electrode. Figure 7 compares the polarization curves for the ORR of RuO_2-based electrodes with those of IrO_2-based and a platinum plate electrodes, and Table 2 presents the E_{ORR} values of these electrodes including the $RuMo(1:1)O_2/Ti$ and $RuV(7:3)O_2/Ti$. As has been discussed in the previous paper [18], the porous $Ir_{0.6}V_{0.4}O_2/Ti$ electrode showed the onset potentials for the ORR to be $E_{ORR} = 0.90$ V and $E_{ORR-20} = 0.86$ V vs RHE and exhibited higher activity than that of a flat Pt plate electrode at 0.8 V (vs RHE), when the current density for the ORR was evaluated with the geometric surface area. This oxide electrode may have a roughness factor of several decades; therefore, the actual effective surface area of this porous oxide electrocatalyst requires evaluation. The catalytic activity for the ORR of the RuO_2-based electrodes is lower than those of IrO_2-based electrodes; however, it is noteworthy that the catalytic activity of RuO_2/Ti electrode for the ORR can be greatly enhanced by the formation of fine RuO_2 particles connecting to each other on the titanium substrate.

Conclusions

As has been discussed in the previous paper [18,19], the porous $Ir_{0.6}V_{0.4}O_2/Ti$ electrode exhibited twice the activity of a flat Pt plate electrode at 0.8 V (vs RHE), when the current density for the ORR was evaluated for the geometric surface area. Although the ORR activity of the La_2O_3-treated RuO_2/Ti was still

lower than the platinum electrode, the enlargement of the surface area of the RuO$_2$/Ti oxide electrode with the help of lanthunum can considerably enhance the catalytic activity of the RuO$_2$/Ti oxide electrode. This modification method of the morphology of the oxide layer must provide useful information on the design of the oxide cathode catalysts using less-expensive elements.

DSA-type electrodes have many advantages: the coating layer is composed of fine oxide particles connected to each other to form a micro/meso porous structure, the titanium substrate is protected from corrosion by the formation of a dense oxide layer at the interface between the porous oxide coating and titanium substrate, and preparation of the electrodes is easy and useful for the search of new electrocatalysts.

Acknowledgments

References

[1] B. Wang, *J. Power Sources*, **152**, 15 (2005).

[2] J-H. Kim, A. Ishihara, S. Mitsushima, N. Kamiya and K-I. Ota, *Electrochim. Acta,* **52**, 2492 (2007).

[3] J. Prakash, D. A. Tryk, W. Aldred and E. B. Yeager, *J. Appl. Electrochem.*, **29**, 1463 (1999).

[4] F. Mazza and S. Trassatti, *J. Electrochem. Soc.*, **110,** 847 (1963).

[5] K. Lee, A. Ishihara, S. Mitsushima, N. Kamiya and K-I. Ota, *Electrochim. Acta*, **49**, 3479 (2004).

[6] E. Claud, T. Addou, J.-M. Latour and P. Aldebert, *J. Appl. Electrochem.*, **28**, 57 (1998).

[7] J. P. Collman, P. S. Wagenknecht and J. E. Hutchison, *Angew. Chem. Int. Ed. Engl.*, **33**, 1537 (1994).

[8] A. Ishihara, K. Lee, S. Doi, S. Mitsushima, N. Kamiya, M. Hara, K. Domen, K. Fukuda, K-I. Ota, *Electrochem. Solid-State Lett.* **8**, A201 (2005) .

[9] Y. Liu, A. Ishihara, S. Mitsushima, N. Kamiya, K-I. Ota, *Electrochem. Solid-State Lett.* **8**, A400 (2005).

[10] K. Kameyama, K. Tsukada, K. Yahikozawa and Y. Takasu, *J. Electrochem. Soc.,* **141**, 643 (1994).

[11] D. S. Gnanamuthu and J. V. Petrocelli, *J. Electrochem. Soc.*, **114**, 1036 (1967).

[12] A. J. Appleby, *J. Electroanal. Chem.*, **27**, 325 (1970).

[13] K. Lee, L. Zhang and J. Zhang, *J. Power Sources*, **165**, 108 (2007).

[14] K. Lee, L. Zhang and J. Zhang, *J. Power Sources*, **170**, 291 (2007).

[15] Y. Takasu, W. Sugimoto and M. Yoshitake, *Electrochemistry*, **75**, 105 (2007).

[16] Y. Murakami, T. Kondo, Y. Shimoda, H. Kaji, K. Yahikozawa, Y. Takasu, *J. Alloys and Compounds* **239**, 111 (1996) .

[17] Y. Murakami, T. Nakamura, X.-G. Zhang, Y. Takasu, *J. Alloys and Compounds* **259**, 19 6(1997).

[18] Y. Takasu, N. Yoshinaga, W. Sugimoto, *Electrochem. Commun.* **10**, 668 (2008).

[19] N. Yoshinaga, W. Sugimoto and Y. Takasu, *Electrochim. Acta* available onlie http://dx.doi.org/10.1016/j.electacta.2008.07.020

Figure captions

Fig. 1   The electrochemical cell and setup

Fig.2   Cyclic voltammograms of the RuO_2/Ti and $RuO_2(Ru:La=1:1)$/Ti electrodes.

Electrodes: (a) RuO_2/Ti and (b) $RuO_2(Ru:La=1:1)$/Ti.

The broken lines indicate measurement in N_2-saturated electrolyte and the solid lines indicate O_2-saturated electrolyte. The current density is presented as current per geometric surface area of the electrodes.

Electrolyte: 0.5 M H_2SO_4 (60 °C). Sweep rate: 5 mV s^{-1}.

Fig. 3   The ORR-current curves of various RuO_2-based electrodes.

Electrodes: (a) RuO_2/Ti, (b) $RuO_2(Ru:La=9:1)$/Ti, (c) $RuO_2(Ru:La=7:3)$/Ti and (d) $RuO_2(Ru:La=1:1)$/Ti. Electrolyte: 0.5 M H_2SO_4 (60 °C). Sweep rate: 5 mV s^{-1}.

Fig. 4   High magnification SEM images of the RuO_2-based electrodes.

Electrodes: (a) RuO_2/Ti, (b) $RuO_2(Ru:La=9:1)$/Ti, (c) $RuO_2(Ru:La=7:3)$/Ti and

(d) RuO_2(Ru:La=1:1)/Ti.

Fig. 5　XRD patterns of the RuO_2/Ti and RuO_2(Ru:La=1:1)/Ti electrodes.

Electrodes: (a) RuO_2/Ti and (b) RuO_2(Ru:La=1:1)/Ti

Lanthanum species was removed by 0.5 M H_2SO_4 at 80 °C. So long as the EDX analysis, the complete removal of the La_2O_3 by the acid treatment was confirmed.

Fig. 6　The ORR-current curves of various RuO_2-based electrodes.

Electrodes: (a) RuO_2/Ti, (b) $RuMo(1:1)O_2$/Ti, (c) $RuV(1:1)O_2$/Ti and (d) RuO_2(Ru:La=1:1)/Ti. Electrolyte: 0.5 M H_2SO_4 (60 °C). Sweep rate: 5 mV s^{-1}.

Fig. 7　The ORR-current curves of various RuO_2- and IrO_2-based electrodes.

Electrodes: (a) RuO_2/Ti, (b) IrO_2/Ti, (c) RuO_2(Ru:La=1:1)/Ti and (d) $IrV(1:1)O_2$/Ti, (e) a Pt plate. Electrolyte: 0.5 M H_2SO_4 (60 °C). Sweep rate: 5 mV s^{-1}.

Table 1   The onset electrode potentials for the ORR on RuO_2-based electrodes.

Potential V (vs RHE)	RuO_2/Ti	RuO_2(Ru:La=9:1)O_x/Ti	RuO_2(Ru:La=7:3)O_x/Ti	RuO_2(Ru:La=1:1)O_x/Ti
E_{ORR-0}	0.73	0.70	0.77	0.83
E_{ORR-20}	0.50	0.65	0.70	0.79

The definition of E_{ORR-0} and E_{ORR-20} is described in the text.

Table 2   The onset electrode potentials for the ORR on RuO_2- and IrO_2-based oxide electrodes.

Potential V (vs RHE)	RuMo(1:1)O_2/Ti	RuV(7:3)O_x/Ti	RuV(1:1)O_x/Ti	IrO_2/Ti	IrMo(1:1)O_2/Ti	IrV(1:1)O_2/Ti[a]	Pt
E_{ORR-0}	0.70	0.65	0.70	0.84	0.87	0.90	0.89
E_{ORR-20}	0.58	0.55	0.58	0.74	0.79	0.86	0.82

The definition of E_{ORR-0} and E_{ORR-20} is described in the text. a) After the acid-treatment, the IrV(1:1)O_2/Ti electrode changed into $Ir_{0.6}V_{0.4}O_2$/Ti due to the partial disslution of vanadium species.

Potentiostat

N$_2$

N$_2$ or O$_2$

Test Electrode

Reference Electrode Ag/AgCl

Lugin Capillary

Counter Electrode (Carbon Felt)

Fig. 1   Y.Takasu et al.

(a)

(b)
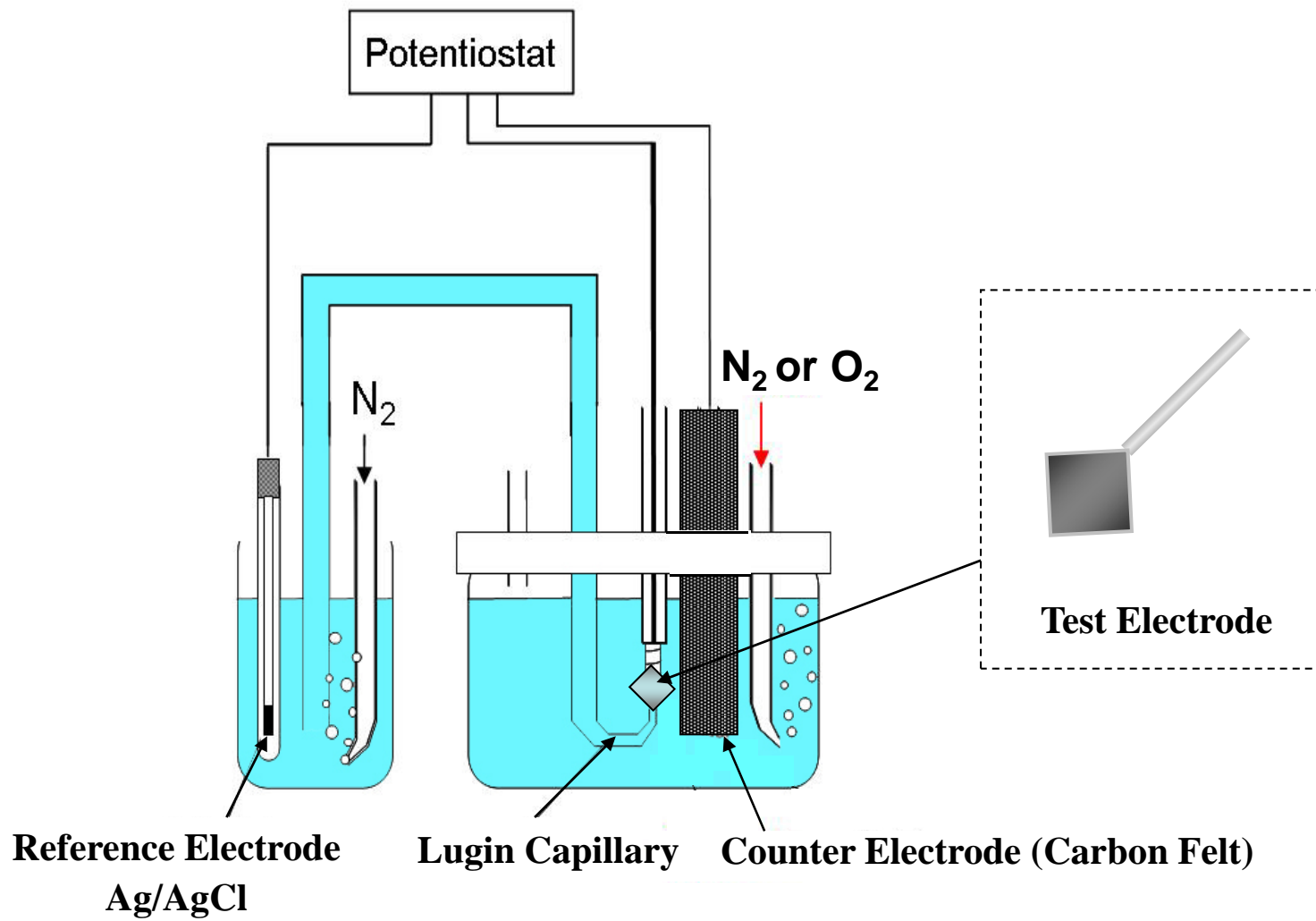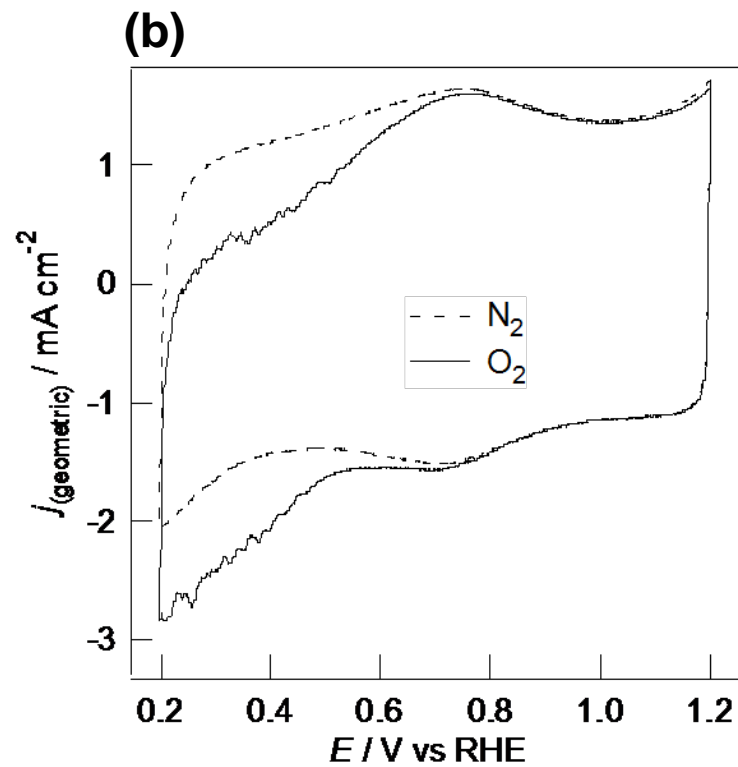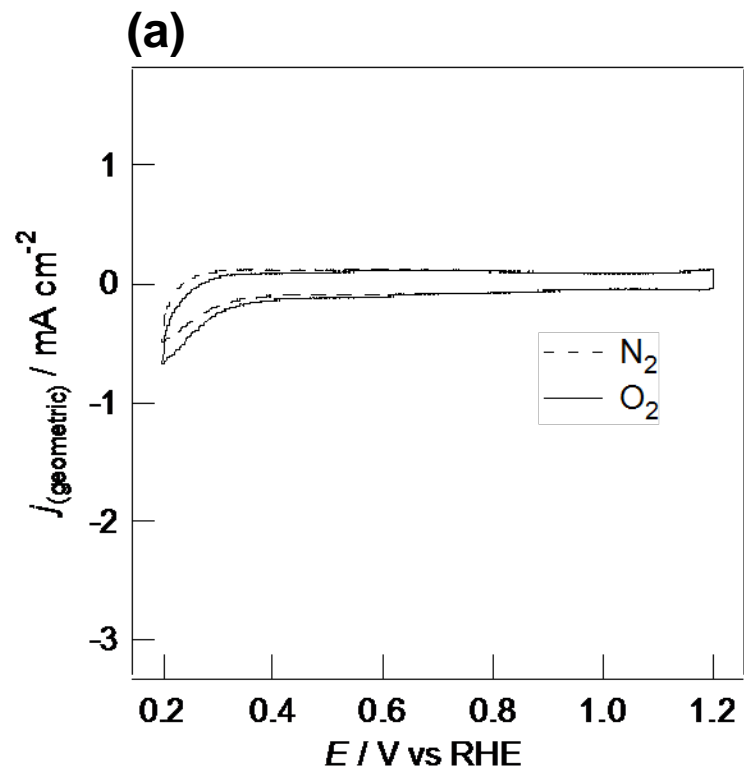
Fig. 2 Y.Takasu et al.

Fig. 3 Y.Takasu et al.

(a) RuO 20.0kV X400K 75.0nm

(b) Ru9La1 20.0kV X400K 75.0nm

(c) Ru7La3 20.0kV X400K 75.0nm

(d) RuLa 20.0kV X400K 75.0nm
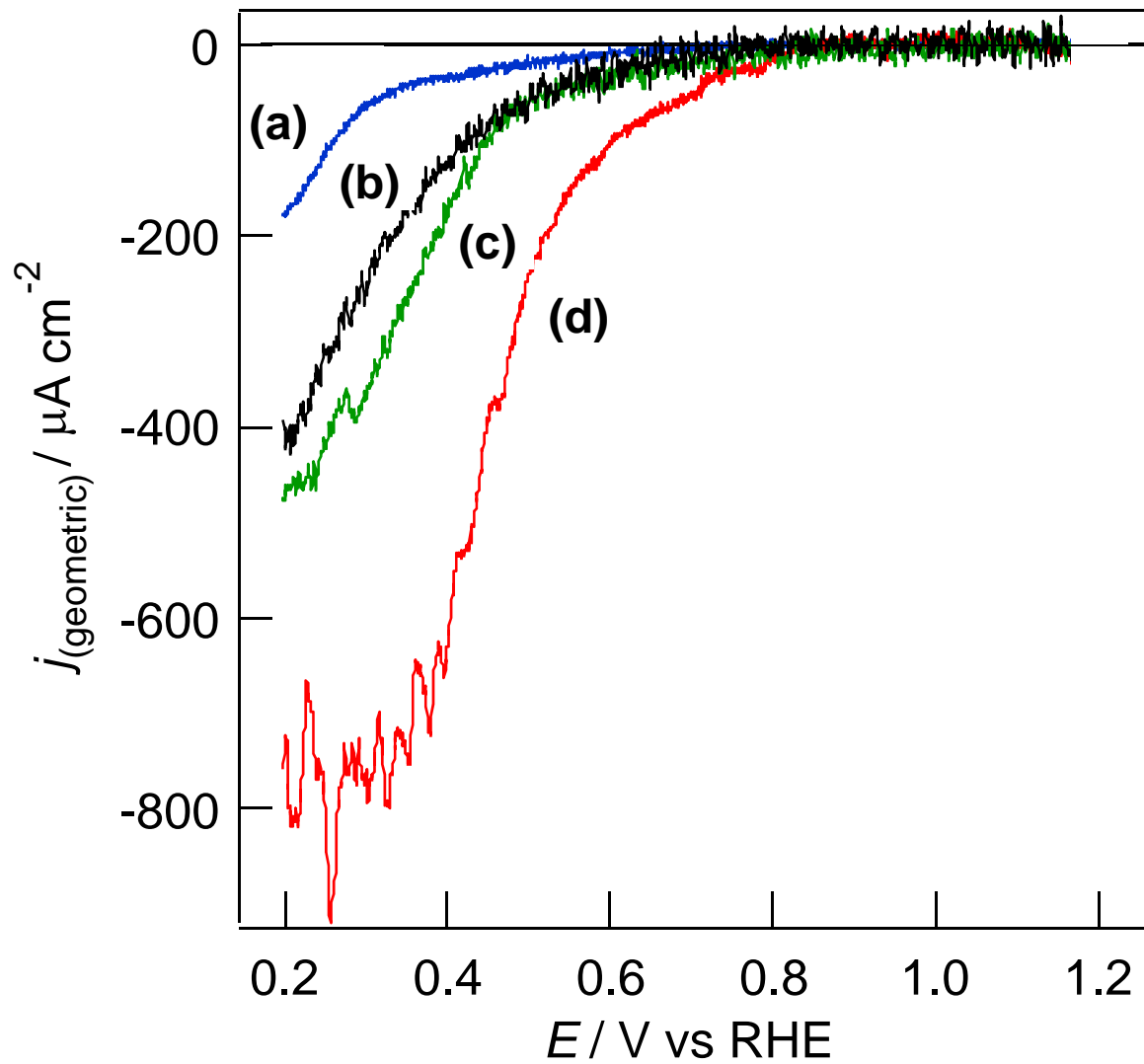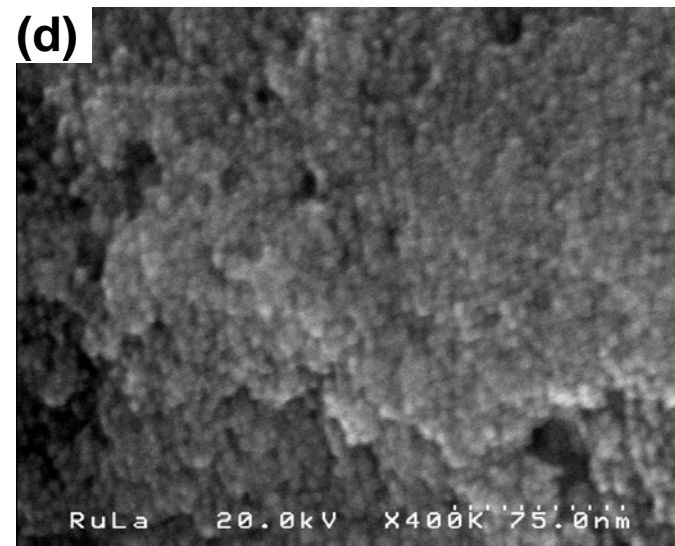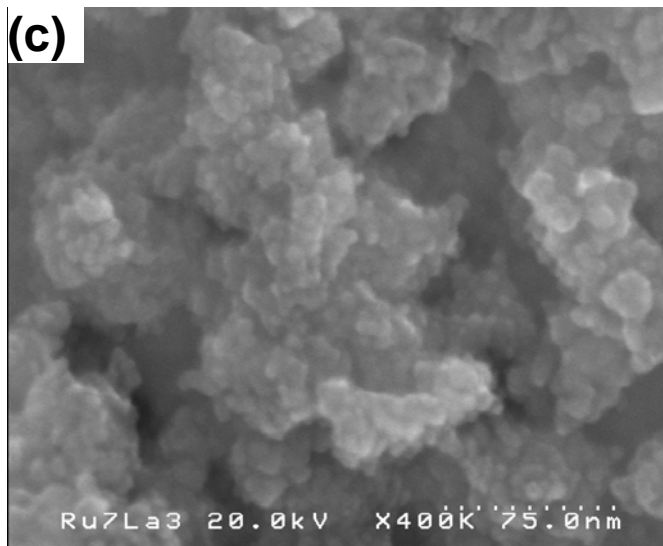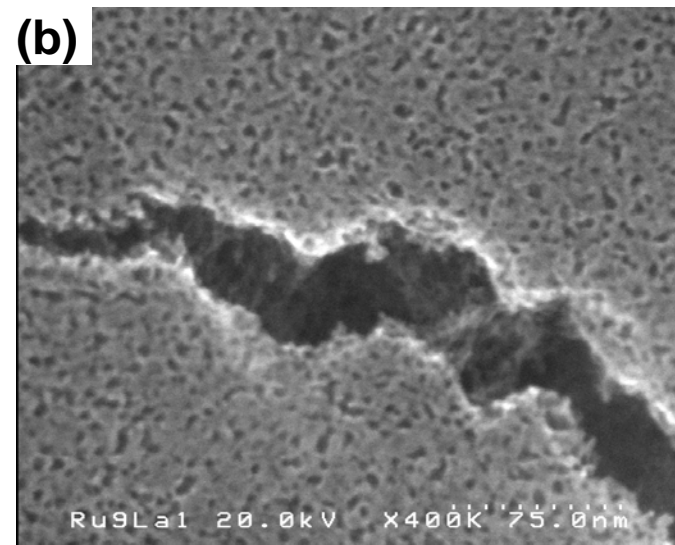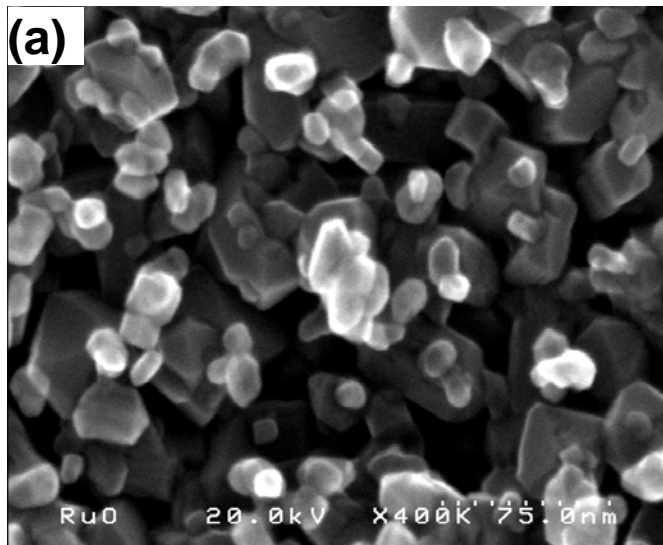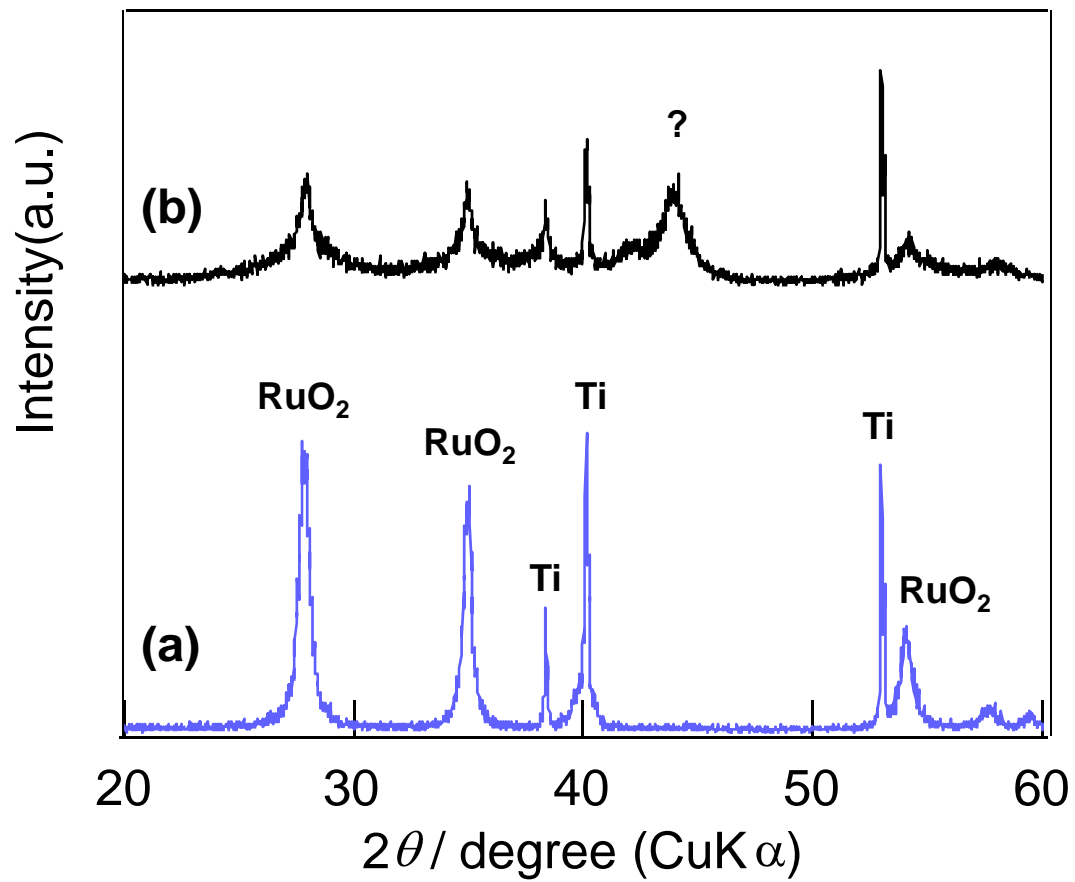
**Fig. 4 Y.Takasu et al.**

Fig. 5 Y.Takasu et al.
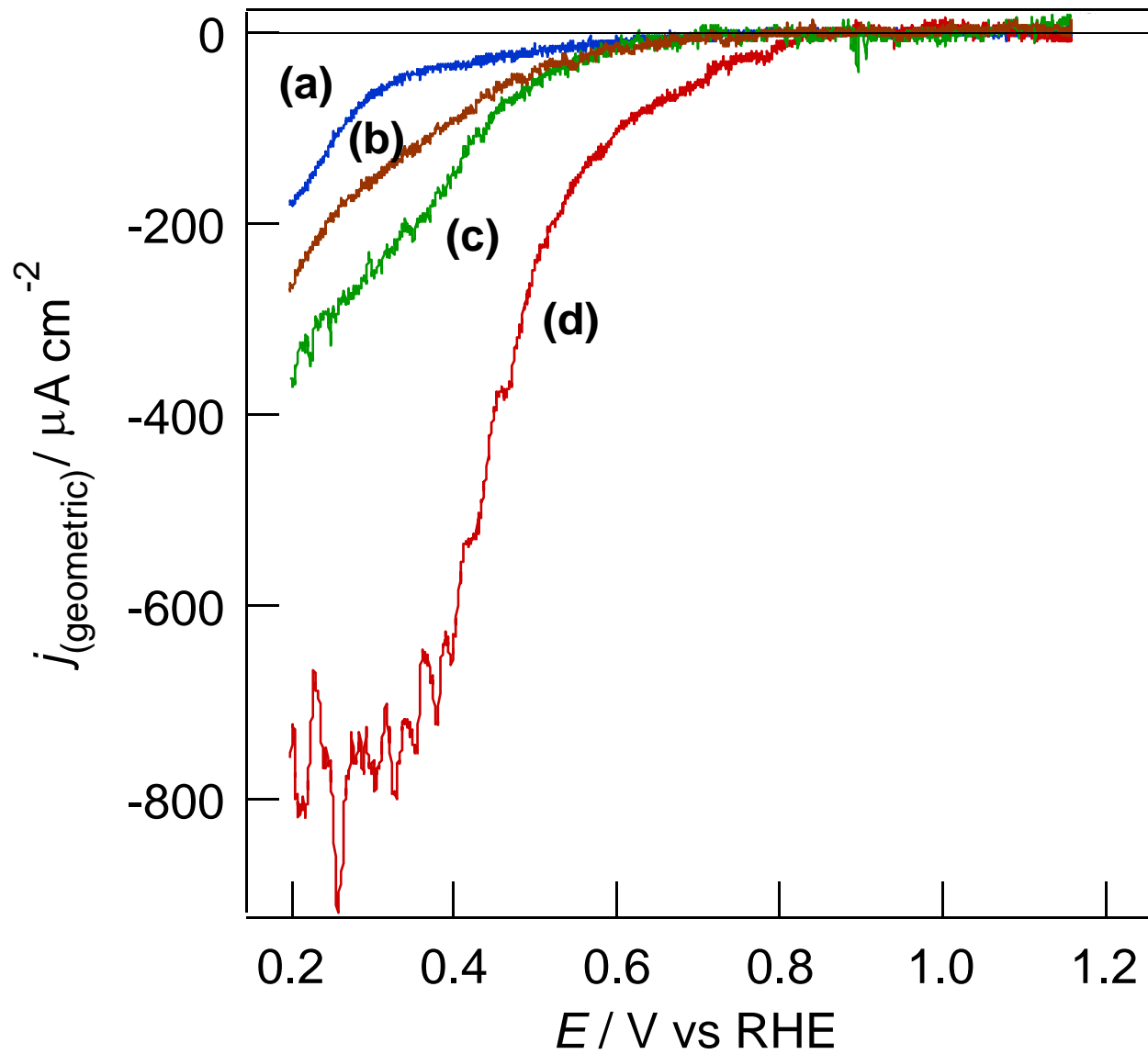
Fig. 6 Y.Takasu et al.

Fig. 7 Y.Takasu et al.